Fire Plume in a Sharply Stratified Ambient Fluid

Samuel Vaux, Rabah Mehaddi, Anthony Collin, Pascal Boulet

Fire Technology manuscript No.
(will be inserted by the editor)

Fire plume in a sharply stratified ambient fluid

Samuel Vaux · Rabah Mehaddi · Anthony Collin · Pascal Boulet

Received: 19 July 2020 / Accepted: 02 February 2021

Highlights:

- Numerical simulations of fire plumes impinging a two-layer stratified environment
- Theoretical model for trapping/escaping fire plume
- Simplified engineering correlation to evaluate the trapping height

Abstract The present work analyses theoretically and numerically fire plumes evolving in a two-layer stratified environment. The ambient fluid consists of a lower cold (heavy) layer and an upper warm (light) layer with a sharp interface. The fire plume is controlled by the fire heat release rate Q. Depending on the density interface location, the temperatures of the layers and on the fire source conditions, the fire plume can rise indefinitely or can be captured by the density stratification. To determine a criterion between these two situations, a theoretical model is proposed. With this model, it is found that the trapping/escaping criterion of the fire plume is determined in terms of a stratification parameter $\Lambda > 0.88$. This stratification parameter Λ is a function of the fire heat release, the density interface location and the ambient stratification. The model also allows the plume height to be determined analytically. The comparison with the numerical data shows an excellent agreement. Finally, for practical purposes, we propose a simplified correlation to estimate the height of the trapped plume as a function of the interface height, the temperatures of the layers and the fire heat release rate.

Keywords Fire plume · Stratification · Fountain · Fire detection

Samuel Vaux
Institut de Radioprotection et de Sûreté Nucléaire (IRSN), PSN-RES, SA2I, LIE,
Cadarache, 13115 Saint-Paul-lez-Durance, France
Tel.:+334 42 199755
E-mail: samuel.vaux@irsn.fr

Rabah Mehaddi · Anthony Collin · Pascal Boulet
Université de Lorraine, CNRS, LEMTA UMR 7563,
54 518 Vandoeuvre-lès-Nancy, France

Nomenclature listing

b	plume width (m)
C	constant
c_p	heat capacity J/(kg.K)
D	diameter of the fire source (m)
E	entrainment of the fountain
F	buoyancy flux (m^4/s^3)
Fr	Froude number
H_l	height of the cold layer (m)
H_f	penetration height of the plume above the interface (m)
q	volume flux (m^3/s)
Q	fire heat release rate (W)
Q_c	convective heat flux (W)
w	plume velocity (m/s)
Re	source Reynolds number
T	temperature (K)

Greek

α	entrainment coefficient of the plume
ϵ	density deficit of the ambient
η	density deficit of the plume
Λ	stratification parameter
ρ	density (kg/m^3)

subscripts

i	interface
l	lower layer
u	upper layer

1 Introduction

In buildings, atria or large rooms are generally equipped with large windows allowing the sun's heat to thermally stratify the inner environment. In this type of configuration, the induced stratification may be approximated by two layers of air of different temperature. In case of fire, the smoke plume can be captured by the stratification, rising to a finite height. Knowing that the smoke detectors are often located at the ceiling, it is then necessary to evaluate their ability to identify the presence of smoke coming from the ground (see [1–3]). The underlying physical processes can be summarized as follows. The buoyant plume, lighter than the lower ambient layer, engulfs ambient fluid due to the turbulent entrainment process, leading to an increase of its mean density (see for instance [4, 5]). When the plume reaches the interface (between the two layers), if its density is larger than the upper layer fluid, the buoyancy is negative (the gravity force acts in the opposite direction to that of the momentum) and a fountain is formed. On the other hand, if the plume density is lower than the density of the upper layer, the resulting buoyancy is positive and the plume rises indefinitely. To determine which of the two possible behaviours arises, it is necessary to determine a separation criterion for the plume trapping/escaping cases. Note that a similar process can be observed in the case of a fire plume developing in a linearly stratified fluid (see for instance [6–11]). Note also that the

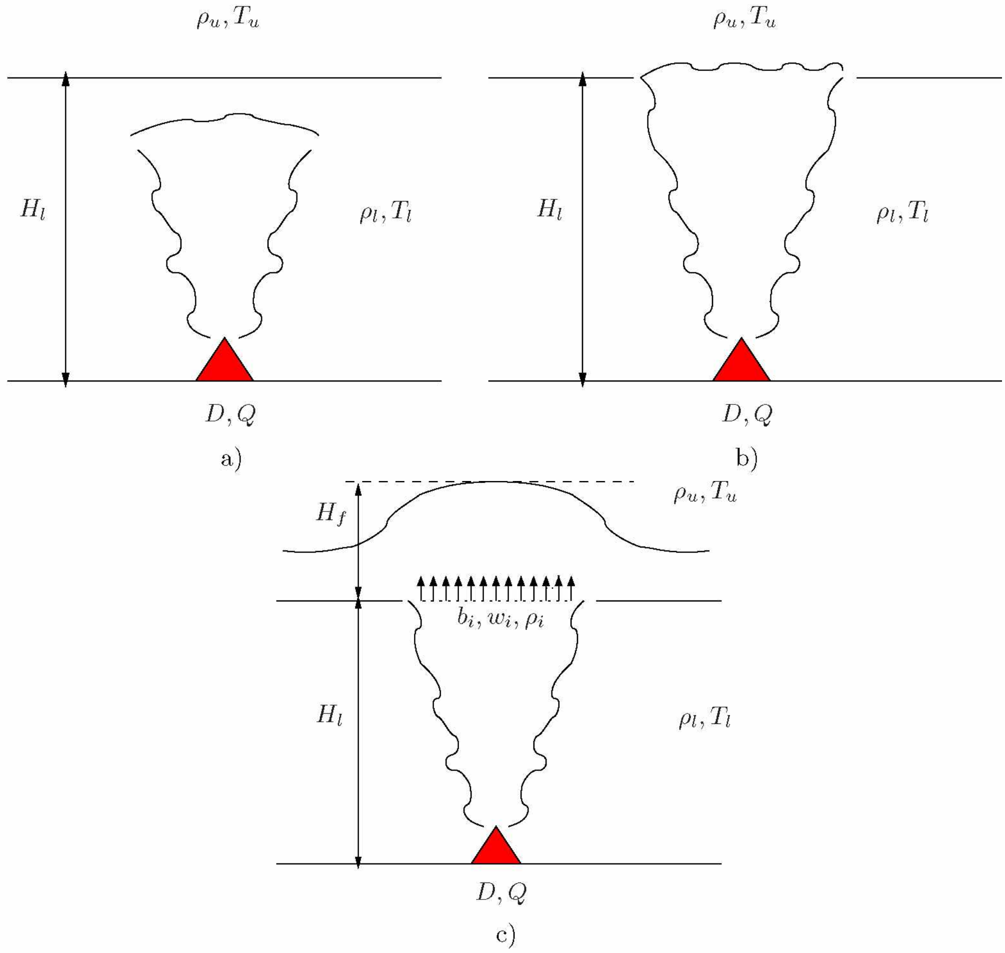

Fig. 1 Schematic of a fire plume developing in a two-layer stratified fluid showing three different stages: (a) the initial rise of the plume in the lower layer, (b) the impingement of the plume on the interface and (c) the development of the steady turbulent fountain above the interface. Also shown are the fire diameter D, the fire heat release rate Q, the lower layer depth H_l, the densities of the lower and upper layers, respectively ρ_l and ρ_u, the temperatures of the lower and upper layers, respectively T_l and Tu, and finally the fountain height H_f above the interface.

same problem appears in ventilation [12] where the objective is to mix the atmosphere of a room in order to achieve a homogeneous temperature.

Plumes developing in a two-layer stratified ambient were the subject of several studies. These studies mainly focused on the penetrative behaviour of the flow at the interface. Particularly, they attempted to quantify the entrainment (mixing) of the resulting flow through an entrainment rate E defined in [13] as $E = q_e/q_i$, where q_e is the volume flux entrained by the emerging fountain in the upper layer, $q_i = \pi b_i^2 w_i$ is the volume flux of the plume at the interface, b_i is the plume radius at the interface and w_i is the velocity at the interface. To quantify the entrainment rate E, Baines [13] used the Froude number Fr, defined at the interface as follows:

$$Fr = \frac{w_i}{\left(g\frac{(\rho_i - \rho_u)}{\rho_u} b_i\right)^{1/2}} , \qquad (1)$$

where $(\rho_i - \rho_u)/\rho_u$ is the density deficit at the density interface. Baines [13] showed experimentally that $E \propto Fr^3$. Later, the experiments by Kumagai [14] extended the range of the interfacial Froude number investigated by Baines [13] and proposed an empirical formula for the entrainment rate E. The entrainment mechanism identified by these authors involves the presence of vortices at the interface that incorporate the upper layer fluid into the fountain [15]. An exhaustive review of the studies focusing on the interaction of fountains with a sharp density interface can be found in [16]. With the aid of a theoretical model, these authors showed that at large Froude numbers, $E \propto Fr$, and at low Froude numbers, $E \propto Fr^2$. Moreover, Shrinivas and Hunt [16] identified a discrepancy between existing experimental data at low values of the Froude number. This discrepancy has been subsequently elucidated in [17] and is related to the confinement of the flow. More recently, a second mechanism of mixing has been identified by Herault *et al.* [18] and this mechanism is due to waves developing at the interface. Concerning the penetration height of the fountain (above the density interface), noted hereafter H_f, it has been quantified by Shy [19] as a function of the interfacial Froude number, namely $H_f/b_i \propto Fr^2$. A similar scaling has been determined experimentally in [20] and [21] and theoretically in [16] for low interfacial Froude number. Finally, and perhaps more importantly, it should be mentioned that most of these studies consider the impact of a jet on a density surface, i.e. the case where the released fluid has a density equal to that of the lower layer. Actually, to our knowledge, very few studies have been reported that investigated the effect of the source conditions of a released plume on the resulting flow at the density interface. In the particular case of a fire source, there are no studies reported in the literature that focus on the fire plume evolving in a two-layer stratified ambient fluid. We can therefore wonder if these kinds of plumes have a similar behaviour to those observed in [13] and [18]. Another issue is how these types of plume evolve, in particular their height, as a function of the fire diameter and the heat release rate.

Therefore, in the present work, our objective is to characterize the development of a fire plume in a two-layer stratified environment according to the fire source conditions and the ambient stratification. To do so, as a first step, the fire plume will be modelled in the lower layer using a theoretical approach based on the plume theory originally developed by Morton *et al.* [22]. Then, at the impact level, we will use some fundamental results on turbulent fountains [23, 24] to quantify the total height of the plume. This is, to the best of our knowledge, the first model to date for this configuration. Secondly, numerical simulations will be carried out in order to verify and reinforce the relevance of the theoretical findings and a simple relation will be finally derived for practical engineering applications.

The paper is organised as follows. In section 2, the theoretical model is presented. In section 3, our numerical model is described and the results of the numerical simulations are presented and compared with the theoretical model in section 4. Finally, the main conclusions are summarized in section 5.

2 Theoretical model

2.1 Determination of the trapping/escaping criterion

The present study considers a fire plume developing in a stable two-layer stratified infinite environment. The densities of the lower and upper layers are respectively denoted ρ_l and ρ_u where $\rho_l > \rho_u$. Note that the corresponding temperatures of the lower and upper layers are similarly denoted T_l and T_u respectively where $T_l < T_u$. Figure (4)c) shows a schematic of the configuration. The buoyant plume issues from a fire with a heat release rate denoted Q and a diameter denoted D. The distance between the buoyant plume source and the interface is denoted H_l. In the lower layer, the plume behaves as a turbulent plume rising in a homogeneous fluid. Owing to the turbulent entrainment [22], the plume progressively incorporates the ambient fluid and, as a consequence, its density rises with the vertical coordinate z. At the interface, if the plume density, denoted ρ_i, is larger than the upper layer density (i.e. $\rho_i > \rho_u$), the plume behaves as a fountain [23, 25]. Actually, at the interface, the plume flow penetrates the upper layer and, due to its negative buoyancy, reverses direction at a certain height which is called hereafter the plume height H_p where $H_p = H_f + H_l$.

To model fire plumes, Morton [26] extended the solutions of weakly buoyant plumes (small density difference) given in [22] to strongly buoyant plumes for which the density difference is large (see Appendix A for similarity solutions of the plume model). In the lower layer, the fire plume variables, namely the radius b, the bulk velocity w and the bulk temperature can therefore be written as follows:

$$b = C_1 \left(\frac{\rho_l}{\rho}\right)^{1/2} z \,, \tag{2}$$

$$w = C_2 F^{1/3} z^{-1/3} \,, \tag{3}$$

$$\eta = C_3 F^{2/3} z^{-5/3} \,, \tag{4}$$

where z is the vertical coordinate, $\eta = (\rho_l - \rho(z))/\rho(z) = (T(z) - T_l)/T_l$ is the density (or temperature) deficit, $\rho(z)$ is the *top-hat* plume density, $T(z)$ is the *top-hat* temperature, and F is the source buoyancy flux of the plume. The buoyancy flux F can be related to the convective heat flux Q_c of the fire source as :

$$F = \frac{g}{\rho_l \, T_l \, c_p} Q_c \,, \tag{5}$$

where g is the gravitational acceleration and c_p is the heat capacity of air. The convective heat flux Q_c is generally taken as a fraction χ of the fire heat release rate Q (i.e. $Q_c = \chi\, Q$). Note that, at the interface, $\eta(H_l)$, $b(H_l)$ and $w(H_l)$ will be noted η_i, b_i and w_i.

In equations (2)-(4), the constants C_n are functions of the entrainment coefficient α

$$C_1 = \frac{6\alpha}{5} \,, \tag{6}$$

$$C_2 = \left(\frac{3}{4}\right)^{1/3} \left(\frac{6\alpha}{5}\right)^{-2/3} \left(\frac{1}{\pi}\right)^{1/3} \,, \tag{7}$$

$$C_3 = \frac{1}{g} \left(\frac{3}{4}\right)^{-1/3} \left(\frac{6\alpha}{5}\right)^{-4/3} \left(\frac{1}{\pi}\right)^{2/3} \,. \tag{8}$$

To observe a turbulent fountain above the interface, the density of the plume fluid must be greater than the upper layer density, i.e. $\rho(H_l) = \rho_i > \rho_u$. This simple condition leads us to :

$$\frac{\rho_l - \rho_u}{\rho_l - \rho_i} > 1 \,, \tag{9}$$

and replacing ρ_i by its expression deduced from equation (4), one arrives at the following relation :

$$\Lambda > C_3 \qquad \text{where} \qquad \Lambda = \frac{\epsilon}{1-\epsilon} \frac{H_l^{5/3}}{F^{2/3}} \quad \text{and} \quad \epsilon = \frac{\rho_l - \rho_u}{\rho_l} \,. \tag{10}$$

If this criterion turns out to be verified, then the plume actually gives rise to a fountain above the interface. In the opposite case, it escapes from the interface and rises indefinitely. In the next section, we focus on the special case where a fountain forms above the interface (namely the trapping case, for which $\Lambda > C_3$) and we look for an estimate of the total plume height H_p based on a theoretical analysis.

2.2 The plume height

In case of trapping, in order to estimate the height of the fountain, we use some fundamental results on turbulent fountains. Indeed, since the pioneering work by Turner [27] and thanks to more recent experiments [23], it is well established that the dimensionless fountain height (divided by the radius of its source) is governed by the source Froude number Fr defined in equation (1). In the present case, the fountain source is located at the interface with radius b_i, velocity w_i and density difference $(\rho_i - \rho_u)/\rho_u$. Using the definition of the parameter Λ and the values of the primary variables b_i, w_i and η_i, the interfacial Froude number can be expressed as follows :

$$Fr = \frac{C_2\, C_3^{1/4}}{(g\, C_1)^{1/2}} \left[\frac{\epsilon}{\Lambda\,(1-\epsilon)} + \frac{1}{C_3}\right]^{1/4} [\Lambda - C_3]^{-1/2} \,. \tag{11}$$

Moreover, the fountain height scales differently depending on the value of the Froude number. Indeed, in the case of forced fountains, corresponding to $Fr > 3$, the fountain height scales as $H_f/b_i \propto (\rho_i/\rho_u)^{3/4}\, Fr$ (see [24]). In the case of weak and very weak fountains, the dimensionless fountain height respectively scales as $H_f/b_i \propto Fr^2$ for $1 < Fr < 3$ and $H_f/b_i \propto Fr^{2/3}$ for $Fr < 1$. Note that, in the very weak regime, the fountain does not have the required momentum to emerge. In that case, $H_f \approx 0$. Replacing b_i and Fr by their respective expressions, we can obtain the fountain height as follows

$$\frac{H_f}{H_l} \propto \frac{C_2 C_1^{1/2}}{g^{1/2}} (1-\epsilon)^{-3/4} (\Lambda - C_3)^{-1/2} \qquad \text{for} \qquad Fr > 3\,, \tag{12}$$

$$\frac{H_f}{H_l} \propto \frac{C_2^2\, C_3}{g} \left[\frac{\epsilon}{\Lambda(1-\epsilon)} + \frac{1}{C_3}\right] [\Lambda - C_3]^{-1} \qquad \text{for} \qquad Fr < 3\,. \tag{13}$$

In the case where the environment is slightly stratified, which means that $\epsilon \ll 1$, the leading orders of equations (12) and (13) can be expressed as follows

$$\frac{H_f}{H_l} \propto \frac{C_2 C_1^{1/2}}{g^{1/2}} (\Lambda - C_3)^{-1/2} + O(\epsilon) \qquad \text{for} \qquad Fr > 3\,, \tag{14}$$

$$\frac{H_f}{H_l} \propto \frac{C_2^2}{g} [\Lambda - C_3]^{-1} + O(\epsilon) \qquad \text{for} \qquad Fr < 3\,. \tag{15}$$

These final relations show that, in the trapping regime, the fountain height is only a function of Λ. In the next section, numerical simulations are carried out in order to verify the theory and to determine the values of the correction factors of these relations.

3 Numerical simulations

To perform the numerical simulation of a turbulent fire plume in a two-layer stably stratified fluid, we use the code CALIF^{3}S-ISIS developed at the French Institut de Radioprotection et de Sûreté Nucléaire (IRSN), originally dedicated to the simulation of fires in mechanically ventilated compartments [28, 29] and more generally to three-dimensional simulations of turbulent and slightly compressible flows (low-Mach-number approach). The Favre-averaged Navier-Stokes equations (mass and momentum balance) along with the heat transport equation are solved. In addition, this averaged process requires closure rules dealt with a turbulence model. To model the Reynolds-stress tensor and turbulent scalar fluxes, we use the eddy viscosity hypothesis and the first order $k-\epsilon$ model with two balance equations. The fire has been modelled as a volumetric source of heat without a dedicated combustion model. This fire modelling constitutes a simplified approach because neither the combustion equation nor the radiation equation are solved. However, it is a relevant and commonly used approach [30, 31] in many practical applications and one of its advantages lies in its low computational cost. For a detailed presentation of the governing balance equations solved by CALIF^{3}S-ISIS software, the reader may consult Appendix A of [32].

We use a staggered grid with a cell-centred piecewise constant representation of the scalar variables and with a marker and cell (MAC) type finite volume approximation for the velocity. For the time discretization, a fractional step algorithm is used decoupling balance equations for the transport of energy and Navier-Stokes equations which are solved by a pressure correction technique. The three-dimensional computational domains Ω are rectangular boxes set to $[-l/2 : l/2]^2 \times [0 : L]$ where l and L are respectively the lateral and the vertical lengths of the domain. In each simulation, the values set to the total lateral l and vertical

L lengths depend on the physical parameters of the flow under consideration (see appendix B for more detail). The volumetric heat source is located on the bottom solid boundary of the computational domain Ω and the resulting fire plume emerges at the center of Ω. A refined Cartesian grid with a uniform square mesh ($\Delta x \times \Delta y$) is used over a subregion $\Omega_1 = [-D; D]$ centred at the origin. Another refined subregion Ω_2 surrounds Ω_1 . Outside Ω_2, the grid is stretched toward the lateral boundaries of the computational domain. In the vertical direction z, the grid spacing (i.e. Δz) is uniform from the bottom boundary up to a vertical distance L_{1z} and then stretched toward the upper boundary. According to the case simulated, different mesh sizes have been used. For each simulated case, a grid convergence study has been performed in order to validate the refinement of the different meshes (see Appendix C for numerical details) as well as the vertical and lateral domain dimensions used in these numerical runs, i.e. the box length l, the domain height L, the extent of the subregions Ω_1 and Ω_2 and L_{1z}. We tested vertical grid spacings $\Delta z/D$ ranging from 0.8 to 0.125 in L_{1z} and horizontal grid spacings $\Delta x/D$ varying from 0.5 to 0.125 in Ω_2. The horizontal grid spacing was kept constant in Ω_1, namely $\Delta x/D = 0.1$. For the time discretization, the use of implicit schemes allows time step sizes for which CFL (Courant-Friedrichs-Lewy) numbers are greater than one. Nevertheless, for each calculation, we have imposed a CFL number close to unity.

Additionally, in order to verify the ability of the code to reproduce an actual turbulent fountain, as is often the case for a plume becoming a fountain when crossing a sharp density interface, a comparison has been carried out by Mehaddi *et al.* [25] with the experiment by Cresswell and Szczepura [33] (hot water injected into a tank of fresh water with $Re = 5000$ and $Fr = 3.1$), by simulating the equivalent downwards injection of hot air into cold ambient air. It has been shown that the computed time-averaged (radial) profiles of velocity, Reynolds stress and density deficit compare well with the experimental data. In addition, the linear scaling of the steady dimensionless height with the Boussinesq source Froude number, orginally found by Turner [27], is fully recovered. Finally, given that fire plumes may exhibit large density differences with the surroundings and might become non-Boussinesq turbulent fountains when crossing a sharp density interface, the software has also to recover the heights of non-Boussinesq turbulent fountains. In [24], the steady state heights of downward non-Boussinesq turbulent fountains, when compared to the experimental data of Mehaddi *et al.* [34] on air-helium turbulent fountains, are also recovered by the simulations, confirming the suitability of the CALIF^{3}S-ISIS software to properly evaluate the heights of non-Boussinesq turbulent fountains.

4 Results

A total of twenty-eight simulations were achieved for fires of diameter 0.3 m $< D <$ 1.0 m exhibiting a constant convective heat flux Q_c varying from 100 kW to 1100 kW. Concerning the environment, it is weakly stratified (ie $\epsilon \ll 1$) with the stratification parameter Λ in the range $0.79 < \Lambda < 6.71$ (see table 1 for the source parameters of the fire plume simulations and the ambient conditions).

Table 1 Parameters of fire simulations (convective heat flux Q_c and diameter D) evolving in a two-layer stratified ambient (temperatures T_l and T_u). H_f corresponds to the penetration height above the interface given by the numerical simulation. Re is the source Reynolds number (see Appendix C for its determination) and N_x, N_y and N_z are the numbers of cells in each direction.

simulation	Q_c (kW)	D (m)	Re	$N_x \times N_y \times N_z$	H_l (m)	T_l (K)	T_u (K)	Λ	H_f (m)
S0	800	0.5	11415	$135^2 \times 180$	15	293.15	313.15	0.79	∞
S00	750	0.5	10702	$135^2 \times 180$	15	293.15	313.15	0.82	∞
S1	100	0.4	1783	$137^2 \times 185$	15	293.15	303.15	1.57	8.5
S2	200	0.3	4756	$127^2 \times 182$	10	293.15	313.15	1.00	10.75
S3	400	0.4	7134	$122^2 \times 172$	15	293.15	323.15	1.88	7.8
S4	500	0.4	8918	$125^2 \times 163$	15	293.15	333.15	2.15	7.9
S5	600	0.4	10702	$116^2 \times 158$	15	293.15	343.15	2.39	7.0
S6	1000	0.4	17836	$117^2 \times 162$	25	293.15	353.15	4.77	6.3
S7	100	1.0	715	$120^2 \times 149$	10	293.15	313.15	1.60	5.6
S8	200	1.0	1426	$120^2 \times 170$	10	293.15	333.15	2.02	4.7
S9	400	1.0	2856	$114^2 \times 179$	10	293.15	333.15	1.27	8.1
S10	500	1.0	3567	$122^2 \times 152$	10	293.15	333.15	1.09	12.3
S11	600	1.0	4280	$117^2 \times 159$	10	293.15	333.15	0.97	14.25
S12	200	0.5	2853	$118^2 \times 176$	10	293.15	313.15	1.01	9.6
S13	300	0.5	4280	$121^2 \times 156$	15	293.15	313.15	1.51	10.2
S14	500	0.5	7134	$123^2 \times 187$	20	293.15	313.15	1.74	9.4
S15	500	0.5	7134	$123^2 \times 153$	25	293.15	313.15	2.52	12.1
S16	500	0.5	7134	$120^2 \times 166$	30	293.15	313.15	3.42	7.7
S17	650	1.0	4637	$125^2 \times 153$	10	293.15	333.15	0.92	18.5
S18	1100	0.4	19620	$120^2 \times 146$	25	293.15	353.15	4.48	6.5
S19	900	0.4	16053	$119^2 \times 160$	25	293.15	353.15	5.12	5.7
S20	800	0.4	14269	$120^2 \times 157$	25	293.15	353.15	5.54	5.1
S21	600	0.4	10702	$123^2 \times 152$	25	293.15	353.15	6.71	4.5
S22	400	0.5	5707	$121^2 \times 161$	30	293.15	313.15	3.97	7.3
S23	600	0.5	8560	$125^2 \times 171$	30	293.15	313.15	3.03	9.3
S24	500	0.4	8918	$120^2 \times 152$	15	293.15	343.15	2.69	6.5
S25	450	0.4	8026	$116^2 \times 149$	15	293.15	343.15	2.89	5.5
S26	500	1.0	3567	$122^2 \times 152$	10	293.15	333.15	1.10	9.2

We only consider cases where the theoretical trapping condition ($\Lambda > C_3$ where $C_3 \simeq 0.88$) is a priori verified except the simulations S0 and S00 for which $\Lambda = 0.79$ and $\Lambda = 0.82$. As can be seen in table 1, this theoretical condition is fully confirmed by the whole set of simulations giving for H_f (see Appendix D for the determination of the steay fountain height) a finite value except for the simulations $S0$ and $S00$ where the plume rises indefinitely. Furthermore, the non-dimensional height H_f/H_l given by the numerical simulations is plotted as a function of Λ in Figure 2.

We clearly observe that the results of the simulations follow a power-law of the type:

$$H_f/H_l = 0.5(\Lambda - C_3)^{-1/2} . \tag{16}$$

This power-law relation has the form of equation (14) provided by the theory, highlighting that the emerging fountain at the density interface behaves like the prediction given for a forced fountain. In a future investigation, the study of the evolution of the interfacial Froude number Fr as a function of Λ would also be useful to establish a clear classification of the emerging fountains.

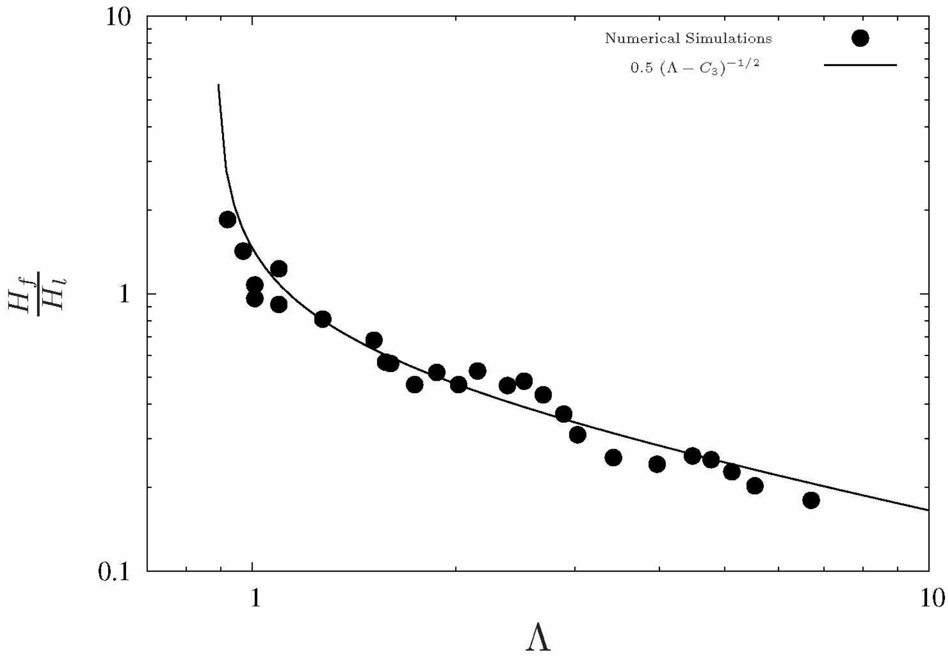

Fig. 2 Comparison between the present model and the numerical simulations made by CALIF[3]S-ISIS code. The black circles correspond to the simulations and the thick-solid line represents equation (16)

For practical fire safety engineering applications, equation (16) can be remodelled, considering the heat capacity c_p as a constant, namely $c_p = 1000$ J/(kg.K), and the product $(\rho_l\, T_l)$ also as a constant (using the ideal gas law). Based on these approximations, a simplified engineering version of equation (16) is written as follows:

$$H_f/H_l = 0.5\left(1090\frac{T_u - T_l}{T_l}\frac{H_l^{5/3}}{Q_c^{2/3}} - 0.88\right)^{-1/2} \tag{17}$$

To illustrate the flow structure of a fire plume impacting a two-layer stratified ambient, we represent in Figure 4 (zoom on the regions of interest, namely the fire plume and the fountain) the non-dimensional temperature $\phi = (T_u - T)/(T_u - T_l)$ and velocity vectors obtained at the steady state for four simulations with increasing values of the stratification parameter Λ. For the simulation S0, where $\Lambda < C_3$, we notice that the impinging plume effectively rises indefinitely in the upper layer. For the three other cases, where $\Lambda > C_3$, we clearly observe that the fire plume, when impacting the density interface, gives birth to an emerging fountain. The upflow of this fountain rises up to the final height H_f and, at this height, an annular downflow settles with a density higher than the surrounding ambient. Simulations also show that at the end of its descent, the downflow changes its direction and goes along the density interface.

5 Conclusions

Fire plumes developing in a two-layer stratified ambient have been studied theoretically and numerically. Starting from the fire plume equations of Morton [26], it is possible to evaluate the primary variables of the fire plume, namely the radius b_i, the velocity w_i and the temperature T_i at the density interface of height H_l.

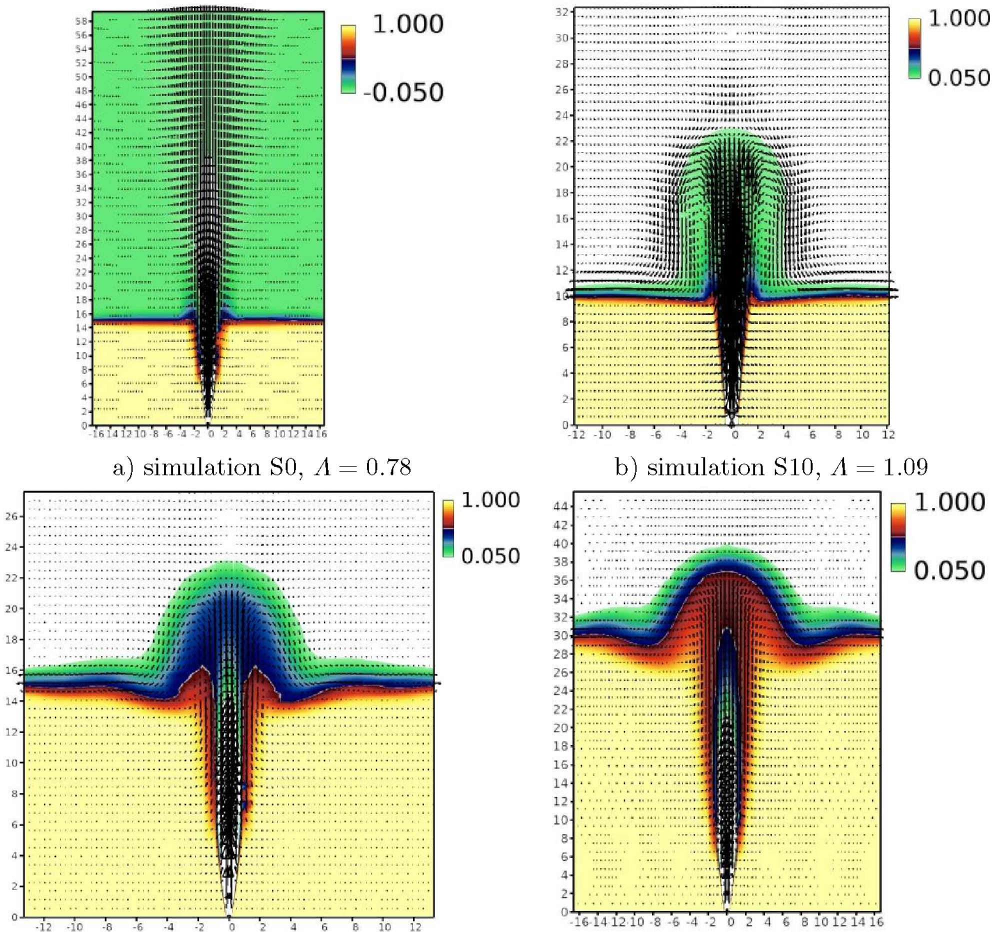

a) simulation S0, $\Lambda = 0.78$ b) simulation S10, $\Lambda = 1.09$

c) simulation S4, $\Lambda = 2.15$ d) simulation S16, $\Lambda = 3.42$

Fig. 3 Visualization of the flow in the vertical median plane for four simulations (a) simulation S0, (b) simulation S10, (c) simulation S4 and (d) simulation S16 corresponding respectively to increasing values of the stratification parameter Λ. The colour bar is scaled by the maximum level of the variable $\phi = (T_u - T)/(T_u - T_l)$ and the minimum level is set to $\phi = 0.05$ (which gives the approximate localization of the emerging fountain) for the trapping cases and $\phi = -0.05$ for the escaping case. Velocity vectors are scaled to give relative velocity magnitude

Then, at this location, following the density of the plume, the emerging plume either continues ascending in the upper layer indefinitely (escaping case) or becomes a fountain (trapping case). In the latter case, based on a simple dimensional analysis exhibiting a stratification parameter Λ and with the help of correlations for the non-dimensional height of turbulent fountains, it is possible to obtain a theoretical non-dimensional height of a trapped plume in a two-layer stratified ambient. When compared to numerical simulations, we observe an excellent agreement between the theoretical estimate and the numerical data. For practical purposes, we also propose a simplified correlation to estimate the height of the trapped plume as a function of the interface height H_l, the temperatures of the layers and the fire heat release rate. Finally and besides the estimate of the height of the trapped plume, it is noteworthy to mention that in large buildings (e.g. warehouses, concert venues,...), fire detectors located on ceilings cannot identify these situations and great care must be taken to fire detection in these configurations. The results obtained in this paper are derived using the assumption of a sharp transition between the lower and upper layers. Usually, the transition is not strictly sharp and the transition between the lower and upper layers may follow a different behaviour. It would be of interest to address this issue in a future work.

A Similarity solutions of the plume model

In this appendix, we briefly recall the main ideas behind the model of Morton *et al.* [22] often referred as the MTT model. These authors proposed a one-dimensional model derived from radial integration of the conservation equations of mass, momentum and buoyancy and this integral model can be written as follows:

$$\frac{d(\rho\, u \pi\, b^2)}{dz} = 2\pi\, b\, \rho_0\, u_e\,, \quad \frac{d(\rho\, u^2 \pi\, b^2)}{dz} = g\,(\rho_0 - \rho)\,\pi\, b^2\,, \quad \frac{d\left(g\,(\rho_0-\rho)\,\pi b^2 u\right)}{dz} = 0\,, \tag{18}$$

where $\rho(z)$, $u(z)$ and $b(z)$ are the top-hat primary variables (along the vertical z-direction) of the plume, namely its density, the vertical component of its velocity and its radius. The variable $u_e(z)$ represents the radial entrainment velocity of ambient fluid of density ρ_0 into the plume and g is the gravitational accelerration. To close the model, an additional relation between u_e and u is specified by:

$$u_e = \left(\frac{\rho}{\rho_0}\right)^{1/2} \alpha\, u\,, \tag{19}$$

where α is the entrainment coefficient. Introducing the variables $\beta = b\,(\rho/\rho_0)^{1/2}$ and $\eta = (\rho_0 - \rho)/\rho$, the conservation equations (18) become as follows:

$$\frac{d(\beta^2 u)}{dz} = 2\alpha\,\beta\, u\, :, \quad \frac{d(\beta^2\, u^2)}{dz} = g\,\eta\,\beta^2\,, \quad \frac{d(g\,\eta\,\beta^2\, u)}{dz} = 0\,. \tag{20}$$

In order to solve equations (20), it is commonly assumed that plume variables evolve as power laws in z, i.e. $\beta(z) = k_\beta\, z^a$, $u(z) = k_u\, z^b$ and $\eta(z) = k_\eta\, z^c$. Introducing these power laws into (20), constants (namely k_β, k_u and k_η) and exponents (namely a, b and c) can be determined to obtain the solutions under the form:

$$\beta = C_1\, z\,, \qquad u = C_2\, F^{1/3}\, z^{-1/3}\,, \qquad \eta = C_3\, F^{2/3}\, z^{-5/3}\,, \tag{21}$$

Introducing the solutions (21) into the conservation equations (20) and noting that $F = \pi\, g\,\eta\,\beta^2\, u$, we finally obtain the equations (6), (7) and (8). By using an entrainment coefficient $\alpha = 0.1$ (see for instance [35]), the value of the coefficients C_1, C_2 and C_3 are given approximately by :

$$C_1 = 0.12\,, \quad C_2 = 2.55\,, \quad C_3 = 0.88\ . \tag{22}$$

B Computational domain dimensions

To choose the dimensions of the computational domains, we use a method close to that adpoted by Vaux *et al.*[24] based on geometrical properties observed in their simulations of turbulent fountains in a uniform ambient fluid. Indeed, for the the maximum height of the fountain and for the radius of the downflow, it has been seen in the literature that these two geometrical characteristics can be exposed as a function of the length scale $\mathcal{L} = b\, Fr$ typical of turbulent forced fountains emerging from a round source of radius b with a Froude number Fr. In the present case, the radius b_i as well as the Froude number Fr_i are the quantities of interest characterizing the emerging fountain at the interface and the length scale is then $\mathcal{L} = b_i\, Fr_i$. To estimate them, we use the relations (2), (3) and (4) at $z = H_l$ to calculate respectively the radius b_i, the

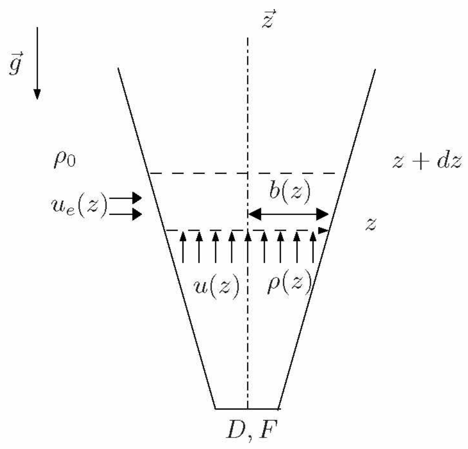

Fig. 4 Schematic of a plume developing in a homogeneous ambient fluid of density ρ_0. The plume emerges from a round source of diameter D with a buoyancy flux F. At a vertcial location z, the entrainment velocity is noted $u_e(z)$ and the plume is characterized by an average density $\rho(z)$, an average velocity $u(z)$ and a radius denoted $b(z)$.

velocity w_i and the density deficit η_i on which Fr_i is built. The total height of the domain, L, is based on the observation, either experimental [23] or numerical [24, 36], that the maximum initial height of the fountain is $H_i/\mathcal{L} \simeq 3.5$. The distance L_{1z} specified in the text corresponds to the initial height H_i of the fountain, i.e. $L_{1z}/\mathcal{L} \simeq 3.5$. Thus, we have chosen $L \simeq 1.33H_i + H_l$, i.e $L \simeq 4.7\mathcal{L} + H_l$. Note that in [36], for the study of turbulent fountains by means of direct numerical simulations, the vertical extent is given by $L/\mathcal{L} = 4.5$. The lateral extent l of the domain is chosen in terms of the radius of the fountain downflow, r_{da}, corresponding to the frontier between the fountain and the ambient fluid. More precisely, we choose values close to that of [36] by considering $(l/2) \simeq 1.75r_{\mathrm{da}}$. In previous simulations [24], it was observed that the fountain radius r_{da} was on average of the order $2\mathcal{L}$ leading to the choice of $l \simeq 7\mathcal{L}$. For its part, the subregion Ω_2 covers the range $[-0.5\mathcal{L} : -D] \cup [D; 0.5\mathcal{L}]$.

C Numerical details

To examine the grid sensitivity of the computed solutions, we focus here on one specific case, namely S4, as an example. For this case, simulations were performed with successively refined grids denoted respectively M1, M2, and M3. M1 is a reference mesh with about 535 000 cells. The mesh M2 is obtained from the mesh M1 by increasing the number of cells in the z direction up to L_{1z} by a factor 2, leading to $8.9\,10^5$ cells. The mesh M3 is obtained from the mesh M2 by increasing the number of cells in the x and y directions leading to about 2.5 million cells. The grid convergence is assessed on the axial profile of the mean vertical velocity $\overline{w}$ of the plume. The results presented in figure 5a) for the case S4 do not show marked differences, except for the maximum velocity in the vicinity of the fire source. We emphasize in particular that, for the major issue under consideration, namely the final steady height of the fire plume H_p, the differences are actually negligible. This is considered as satisfactory for simulations of fire plume in a sharply stratified ambient. Furthermore, we refer the reader to [37] and [38] for the sensitivity analysis and the validation of the CALIF3S-ISIS code. Convergence was considered to be reached as soon as the variations of the mean field fall below 3% of the value of the mean. The duration times of the simulations have been set to values sufficiently large to guarantee first that the steady-states of the fountains are reached and secondly to ensure the convergence of the time-averaged values of the plume variables. As an example, we represent in Figure 5b) the axial profile of the mean vertical velocity $\overline{w}$ for six successive times of the flow development and we note that the convergence is reached from $t = 70\,s$. Actually, for this case, the duration time of the simulation has been set to $T = 100\,s$ given that the time estimated to reach the steady state is $t_{ss} = 20s$ and the time interval over which the statistics were computed has been set to $[25s : 100s]$.

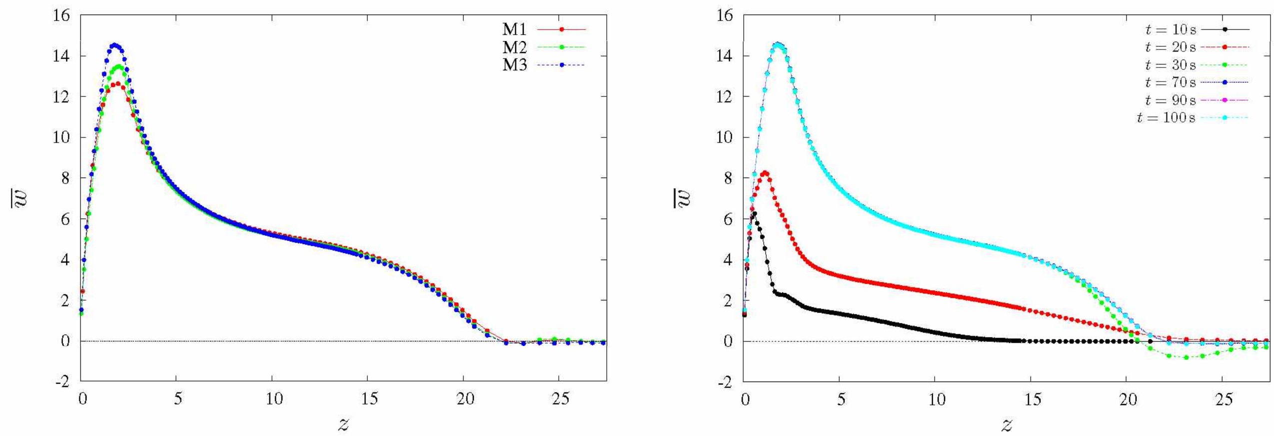

a) b)

Fig. 5 Axial profile of the vertical velocity component $\overline{w}$ for the simulation S4 a) for three grid meshes M1, M2, and M3 at steady state b) at different times for the mesh M3.

In order to determine the Reynolds number Re at the source induced by the fire, we employ a method similar to that of Jiang *et al.*[39]. In their paper, they consider the full combustion of a generic fossil fuel $C_xH_yO_z$. For given values of the heat release rate and of the round source area, they first evaluate the mass flow rate of fuel $\dot{m}_f$ together with the mass flow rate of air $\dot{m}_{\mathrm{air}}$ required for a full combustion to occur. Then, they deduce the temperature rise from the enthalpy of combustion and the associated density ρ_s at the source is given by the ideal gas law. They finally calculate the velocity at the source with the simple relation $w_s = (\dot{m}_f + \dot{m}_{\mathrm{air}})/\rho_s\,A$. In table 1, the Reynolds number $Re = \rho_s\,w_s\,D/\mu$ (where μ is the dynamic viscosity) is considered for the full combustion of propane C_3H_8.

D Determination of the steady fountain height

The criterion for the determination of the steady fountain heights H_f listed in table 1 (for the radial distance $r = 0$) is the null mean vertical velocity at the top of the fountain, i.e. $\overline{w} = 0$. Another criterion based on the temperature can also be used, namely $\phi = (T_u - T)/(T_u - T_l)$ and its use is illustrated in figure 4 with the choice $\phi = 0.05$ giving the approximate localization of the emerging fountain and in particular the position of the steady height H_f. In their study of upward forced turbulent thermal fountains in a uniform ambient by direct numerical simulations, Williamson *et al.*[36] introduce a close criterion, namely $\Phi = (T - T_\infty)/(T_s - T_\infty)$ (where T_s is the source temperature) and they consider in practice the value $\Phi = 0.1$ to identify the top of the fountain. We mention that the values of H_f found either by the criterion based on the null mean vertical velocity or by the temperature criterion ϕ are very close.

References

1. Jun Fang, Ji Jie, Yuan Hong-Yong, and Zhang Yong-Ming. Early fire smoke movements and detection in high large volume spaces. *Building and Environment*, 41(11):1482–1493, 2006.

2. Cristian Maluk, Michael Woodrow, and Jose Luis Torero. The potential of integrating fire safety in modern building design. *Fire Safety Journal*, 88:104–112, 2017.

3. Steve Kerber and James A Milke. Using FDS to simulate smoke layer interface height in a simple atrium. *Fire Technology*, 43(1):45–75, 2007.

4. Gunnar Heskestad. Fire plumes, flame height, and air entrainment. In *SFPE handbook of fire protection engineering*, pages 396–428. Springer, 2016.

5. Gabriele Vigne, Candido Gutierrez-Montes, Alexis Cantizano, Wojciech Wegrzynski, and Guillermo Rein. Review and validation of the current smoke plume entrainment models for large-volume buildings. *Fire Technology*, 55(3):789–816, 2019.

6. G. Heskestad. Note on maximum rise of fire plumes in temperature-stratified ambients. *Fire Safety Journal*, 15(4): 271–276, 1989.

7. G. Heskestad. Fire plume behavior in temperature-stratified ambients. *Combustion Science and Technology*, 106(4-6): 207–228, 1995.

8. Pablo Ayala, Alexis Cantizano, Guillermo Rein, Gabriele Vigne, and C Gutiérrez-Montes. Fire experiments and simulations in a full-scale atrium under transient and asymmetric venting conditions. *Fire Technology*, 52(1):51–78, 2016.

9. Jun Fang and Hong-Yong Yuan. Experimental measurements, integral modeling and smoke detection of early fire in thermally stratified environments. *Fire Safety Journal*, 42(1):11–24, 2007.

10. A.W. Woods. Turbulent plumes in nature. *Annual Review of Fluid Mechanics*, 42:391–412, 2010.

11. R. Mehaddi, F. Candelier, and O. Vauquelin. Naturally bounded plumes. *Journal of Fluid Mechanics*, 717:472–483, 2013.

12. P. Linden. The fluid mechanics of natural ventilation. *Annual Review of Fluid Mechanics*, 31:201–238, 1999.

13. W.D. Baines. Entrainment by a plume or jet at a density interface. *Journal of Fluid Mechanics*, 68(2):309–320, 1975.

14. M. Kumagai. Turbulent buoyant convection from a source in a confined two-layered region. *Journal of Fluid Mechanics*, 147:105–131, 1984.

15. P.F. Linden. The interaction of a vortex ring with a sharp density interface: a model for turbulent entrainment. *Journal of Fluid Mechanics*, 60(3):467–480, 1973.

16. A.B. Shrinivas and G.R. Hunt. Unconfined turbulent entrainment across density interfaces. *Journal of Fluid Mechanics*, 757:573–598, 2014.

17. A.B. Shrinivas and G.R. Hunt. Confined turbulent entrainment across density interfaces. *Journal of Fluid Mechanics*, 779:116–143, 2015.

18. J. Herault, G. Facchini, and M. Le Bars. Erosion of a sharp density interface by a turbulent jet at moderate Froude and Reynolds numbers. *Journal of Fluid Mechanics*, 838:631–657, 2018.

19. S.S. Shy. Mixing dynamics of jet interaction with a sharp density interface. *Experimental Thermal and Fluid Science*, 10(3):355–369, 1995.

20. A.J. Cotel, J.A. Gjestvang, N.N. Ramkhelawan, and R.E. Breidenthal. Laboratory experiments of a jet impinging on a stratified interface. *Experiments in Fluids*, 23(2):155–160, 1997.

21. C.Y. Ching, H.J.S. Fernando, and Y. Noh. Interaction of a negatively buoyant line plume with a density interface. *Dynamics of Atmospheres and Oceans*, 19(1-4):367–388, 1993.

22. B.R. Morton, G. Taylor, and J.S. Turner. Turbulent gravitational convection from maintained and instantaneous sources. In *Proceedings of the Royal Society of London A: Mathematical, Physical and Engineering Sciences*, volume 234, pages 1–23. The Royal Society, 1956.

23. H.C. Burridge and G.R. Hunt. The rise heights of low-and high-Froude-number turbulent axisymmetric fountains. *Journal of Fluid Mechanics*, 691:392–416, 2012.

24. S. Vaux, R. Mehaddi, O. Vauquelin, and F. Candelier. Upward versus downward non-Boussinesq turbulent fountains. *Journal of Fluid Mechanics*, 867:374–391, 2019.

25. R. Mehaddi, S. Vaux, F. Candelier, and O. Vauquelin. On the modelling of steady turbulent fountains. *Environmental Fluid Mechanics*, 15(6):1115–1134, 2015.

26. B.R. Morton. Modeling of fire plumes. In *10 th Symposium (Int.) on Combustion*, pages 973–982. The Combustion Institute, 1965.

27. J.S. Turner. Jets and plumes with negative or reversing buoyancy. *Journal of Fluid Mechanics*, 26(04):779–792, 1966.

28. S. Suard, M. Forestier, and S. Vaux. Toward predictive simulations of pool fires in mechanically ventilated compartments. *Fire Safety Journal*, 61:54–64, 2013.

29. S. Vaux, H. Pretrel, and L. Audouin. Experimental and numerical study of water spray system for a fire event in a confined and mechanically ventilated compartment. *Fire and Materials*, 43(5):579–590, 2019.

30. X. Hue, J.C. Ho, and Y.M. Cheng. Comparison of different combustion models in enclosure fire simulation. *Fire Safety Journal*, 36:37–54, 2001.

31. F. Colella, G. Rein, V. Verda, and R. Borchiellini. Multiscale modeling of transient flows from fire and ventilation in long tunnels. *Computers and Fluids*, 51(1):16–29, 2011.

32. *ISIS 5.8.0.: Physical Modelling. Institut de Radioprotection et de Sûreté Nucléaire, https://gforge.irsn.fr/gf/project/isis/.*

33. R.W. Cresswell and R.T. Szczepura. Experimental investigation into a turbulent jet with negative buoyancy. *Physics of Fluids A: Fluid Dynamics (1989-1993)*, 5(11):2865–2878, 1993.

34. R. Mehaddi, O. Vauquelin, and F. Candelier. Experimental non-Boussinesq fountains. *Journal of Fluid Mechanics*, 784, 2015.

35. Ghislain Michaux and Olivier Vauquelin. Solutions for turbulent buoyant plumes rising from circular sources. *Physics of Fluids*, 20(6):066601, 2008.

36. N. Williamson, S. W. Armfield, and Wenxian Lin. Forced turbulent fountain flow behaviour. *J. Fluid Mech.*, 671: 535–558, 2011.

37. S. Suard, C. Lapuerta, A. Kaiss, and B. Porterie. Sensitivity analysis of a fire field model in the case of a large-scale compartment fire scenario. *Num. Heat Trans., Part A*, 63:879–905, 2013.

38. S. Suard, A. Koched, H. Pretrel, and L. Audouin. Numerical simulations of fire-induced doorway flows in a small scale enclosure. *Int J Heat Mass Trans.*, 81:578–590, 2015.

39. L. Jiang, M. Creyssels, A. Mos, and P. Salizzoni. Critical velocity in ventilated tunnels in the case of fire plumes and densimetric plumes. *Fire Safety Journal*, 101:53–62, 2018.